

AE detection for brazing process at high temperature using an optical fiber AE monitoring system

*Hideo CHO^{1,3)}, Tomoharu HAYANO^{1,4)}, Takuma MATSUO^{2,5)}
and Hiroaki ITO^{1,6)}

¹⁾ *College of Science and Engineering, Aoyama Gakuin University, 5-10-1 Fuchinobe, Sagami-hara, Kanagawa 252-5258, Japan, ³⁾ cho@me.aoyama.ac.jp*

²⁾ *School of Science and Technology Meiji University, 1-1-1 Mita, Taka-ku, Kawasaki, Kanagawa 214-8571, Japan*

ABSTRACT

In this study, we aim to evaluate the bond quality of brazing at high temperatures in vacuum using a heat-resistant optical fiber acoustic emission (AE) monitoring system based on homodyne interference. Because the system is designed for brazing in high-temperature vacuum environments, the heat-resistant fiber was fabricated by plating the Ni-P layer on a commercially available metal-coated fiber, which enables us to monitor AE at temperatures of up to 1150 °C. AE signals can be detected using the system during brazing at appropriate and lower temperatures with a pressure of 2 Pa. These signals are classified into two types based on their frequency characteristics: AE with low-frequency components and AE with broadband frequency components. AE with low-frequency components was detected during both heating and cooling and could be identified as friction noise in the sample and/or a sample holding device. AE with broadband frequency components was detected only during cooling for the low temperature-treated sample and could be caused by poor bond quality.

1. Introduction

Acoustic emission (AE) monitoring is one of potential methods for inspecting manufactured products and monitoring the integrity of bearings (Choudhry 2000), cutting tools (Hase 2014), and infrastructure—such as bridges and oil storage tanks—and it works by detecting elastic waves emitted from microcracks. Because of its high sensitivity and easy handling, a PZT element is used in the AE sensor. However, PZT has a Curie point of approximately 300 °C, above which it loses its piezoelectricity. Therefore, at high temperatures, a waveguide or cooling device is essential for maintaining the sensor at temperatures below the Curie point. Unfortunately, these

³⁾ Professor ⁴⁾ Graduate student ⁵⁾ Associate professor, ⁶⁾ Assistant professor

devices reduce the amplitude of AE and complicate detected AE waveforms because of the dispersive nature of the waveguide rod. Noma et al. (2007) developed a heat-resistant AE sensor with an aluminum nitride (AlN) thin film and succeeded in monitoring AE at high temperatures of up to 1200 °C. Moreover, the sensor requires heat-resistant electrical parts, such as cables, connectors, and a bonding agent between the AlN element and a front plate of the sensor.

On the other hand, an optical fiber sensor is allowed to sense and deliver signal components. Some researchers (Xu 2005, Fomtichov 2002) have reported the use of heat-resistant optical fiber sensors because the optical fiber is made of silica, whose melting temperature is approximately 1500 °C. These heat-resistant sensors were allowed to work below 700 °C. By using electroless Ni plating on a commercially available Cu-coated optical fiber to improve its heat-resistance (Hayano, 2007), our research group has also developed an optical fiber AE monitoring system and succeeded in detecting AE caused by the fracture of oxide scales on carbon steel pipes at temperatures of 600 °C.

In this study, we monitor AE during the brazing process in vacuum under temperatures of up to 1150 °C for in situ evaluation of bond quality with Ni plating on the Cu-coated optical fiber. For the bonding integrity of brazing products, ultrasonic testing at room temperature is performed only after the brazing process. Therefore, in situ monitoring would potentially be required to optimize the heating condition during the process.

2. System and setup

Figure 1 shows the experimental and sample setups used in the study. A heat-resistant optical fiber AE monitoring system is composed of an interferometer and feedback control portions. In the interferometer, a diode laser with a wavelength of 1.55 μm was used as a light source. Emitted light from the laser was split into two beams, which were propagated in the sensing and reference fibers. The sensing fiber was plated with a non-electric Ni-P layer on a commercially available heat-resistant optical fiber with copper as the outermost layer.

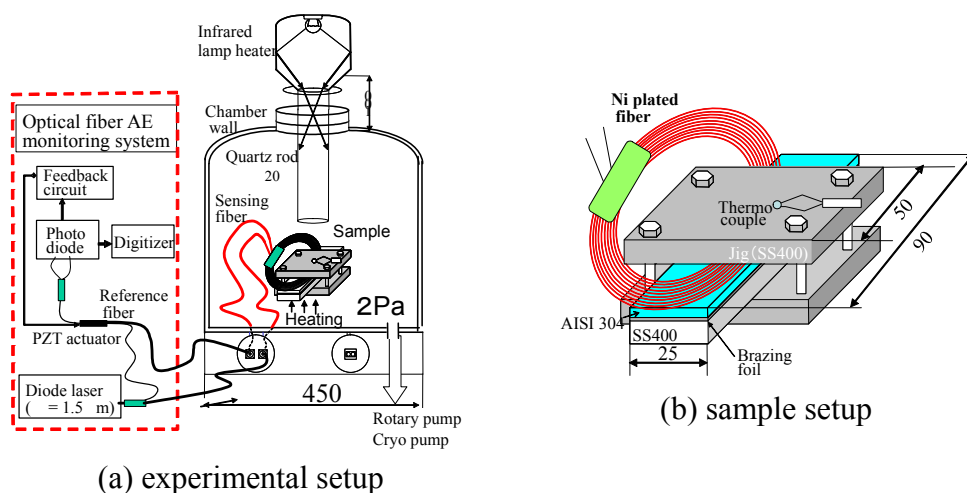


Fig. 1 Schematic of the experimental and sample setups

Figure 2 shows a cross-section of the Ni-P coated fiber, and EPMA analysis for oxygen and Ni components on the cross-section after heat treatment at 600 °C for 450 h. The Ni-P and Cu layers were approximately 5 μm and 20 μm thick, respectively. The oxygen component, which appears as the bright area in Fig. 2(b), existed both on the surface area of the Ni-P layer and inside an optical fiber made of SiO₂. The thickness of oxygen layer in the Ni-P layer was much smaller than that of the Ni-P layer, as shown in Fig. 2(c), and we confirmed that the Ni-P layer behaved as a superior oxidization barrier. Moreover, there was no breakage in the fiber with the Ni-P layer, and the fiber's heat resistance was remarkably improved by the Ni-P layer. The Ni-P coated sensing fiber was shaped as a loop with an inner diameter of 56 mm and placed on the sample sandwiched between two steel plates, as shown in Fig. 1(b), in a vacuum chamber via a specially designed connection flange. When AE signals reached the sensing fiber on the sample, the length of the sensing fiber expanded and shrunk due to the vibration of the sample surface associated with AE, and a phase of light that propagated in the sensing fiber was modulated. The modulated light was interfered by another light propagating in the reference fiber, and then a power change in the interference beam was detected with two photo diodes. To realize system stability, a compensation signal was created with a part of the signal from the diodes after processing with a specially designed electronic circuit and was applied to a PZT actuator that was attached to the reference fiber. The main signal from the diodes was digitized with a PC equipped with an A/D converter after passing a low-pass filter with a cut-off frequency of 200 kHz. A detailed description of the system has been reported in previous papers (Cho (2005) and Cho (2006)).

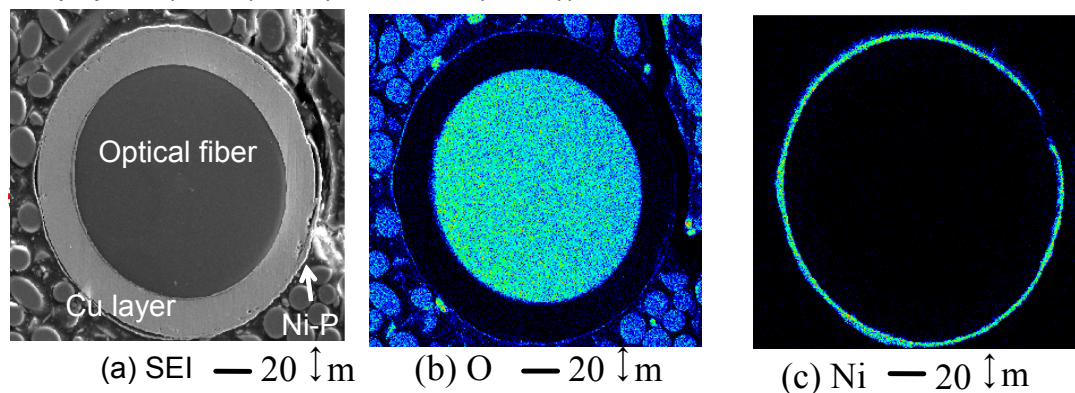


Fig. 2 Cross-section of the developed Ni-P coated fiber and EPMA analysis for O and Ni components on the cross-section after heat treatment at 650 °C for 450 h

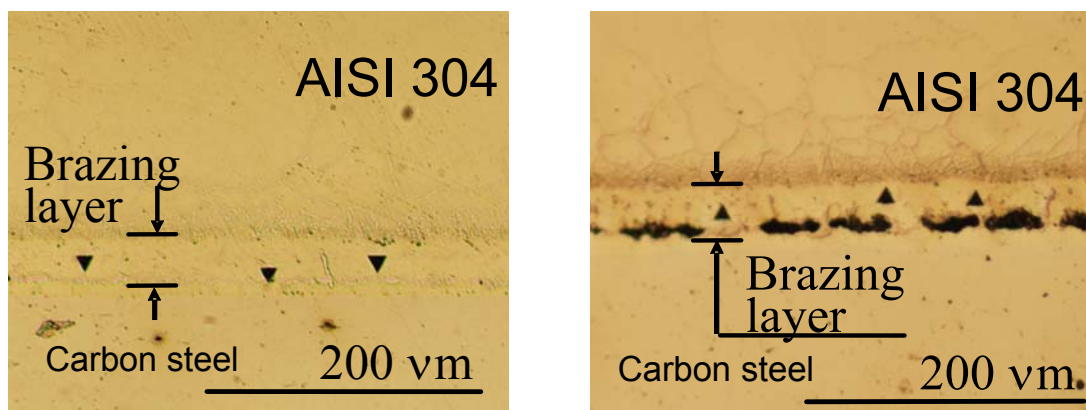
The sample was composed of a 1 mm thick AISI 304 plate, a 10 mm thick carbon steel plate (JIS:SS400), and a 50 μm thick Ni-based amorphous brazing foil (76% Ni, 14% Cr, and 10% P). The width and length of each plate were 90 mm × 25 mm. The brazing foil was inserted between the carbon steel plate and AISI plate and was pressed with two thick carbon steel plates fastened with four bolts. The sample was placed in a vacuum chamber, where the pressure was reduced to 2 Pa, and an electronic heater and infrared lamp heated the sample in the chamber. The temperature was maintained at 1150 °C (proper brazing temperature) for one hour or at 950 °C for one hour for realizing poor bond quality in brazing. The AE signal was

monitored throughout the brazing process; moreover, cross-section observation and an indentation test for the brazing layer were also performed for investigating the brazing layer's bond quality.

3. Experimental results

3.1 Cross-section observation and indentation testing

Figure 3 shows optical images of the cross-sections of each sample after brazing. Triangles in the photos indicate dents made by the indentation test, which was conducted with a Berkovich indenter. In the high-temperature-treated sample, the interface lines between the brazing layer and adherends were not clear, and there were no cracks in the sample. On the other hand, in the low-temperature-treated sample, there were many connecting voids on the interface between the brazing layer and the carbon steel plate adherend, indicating that the bonding quality condition was worse than in the high-temperature sample.



(a) Heat treatment at 1150 °C

(b) Heat treatment at 950 °C

Fig.3 Cross-section of the interface area for the each sample

To check the bonding quality of the brazing layers, an indentation test was performed for the layers in both the samples using a Berkovich indenter with a face angle of 115°. Figure 4 shows five times averaged indentation force–penetration depth curves for each sample. The maximum load was 200 mN. The penetration depth in the high-temperature-treated sample was slightly shallower than that in the low-temperature-treated sample, indicating that the brazing layer in the high-temperature sample was harder. An apparent elastic modulus of the brazing layer, estimated from the elastic unloading stiffness in Fig.4 (which is defined as a slope of the initial portion of the unloading curve) was 55 GPa in the high-temperature sample and 41 GPa in the low-temperature sample. Smaller hardness and elastic modulus values in the low-temperature sample are caused by voids in the interface between the brazing layer and the AISI 304 plate and thus indicates that the bonding quality is low. Hence, the high-temperature-treated sample will be called the well-bonded sample and the low-temperature-treated sample, the weak-bonded sample.

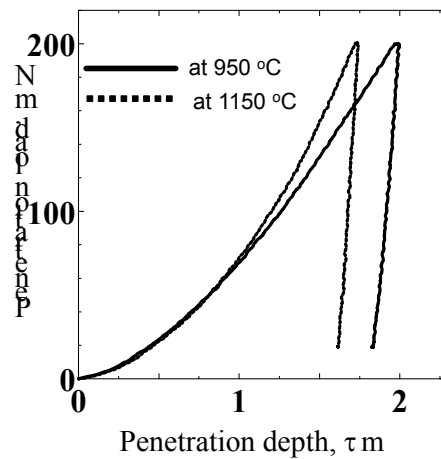


Fig. 4 Load–penetration depth diagrams for each sample, obtained using an indentation test with a Berkovich indenter

3.2 AE monitoring

Two types of AE signals were detected during brazing and were classified according to their frequency characteristics, as shown in Fig. 5. The AE shown in Fig. 5(a) has only low-frequency components below 40 kHz, and the AE shown in Fig. 5(b) has broadband components of 20–120 kHz. Figure 6 shows the cumulative count of each type of AE for the (a) well-bonded and (b) weak-bonded samples and temperature histories. In the well-bonded sample, only low-frequency AE signals were detected during both heating and cooling periods; there were 25 low-frequency AE events. Meanwhile, in the weak-bonded sample, low-frequency AE signals were also detected during both the heating and cooling processes for a total of 49 low-frequency AE events. Broadband AE signals were detected only during the cooling period, and there were 38 broadband AE events. The amplitude of the broadband AE was almost the same as that of the low-frequency AE. Because broadband AE signals were detected only during the cooling process in the sample that had voids along the brazing interface, we can determine that these AEs were related to the voids and could be produced by creating microcracks between these voids due to thermal stress during the cooling process. On the other hand, because low-frequency AEs were detected during both the

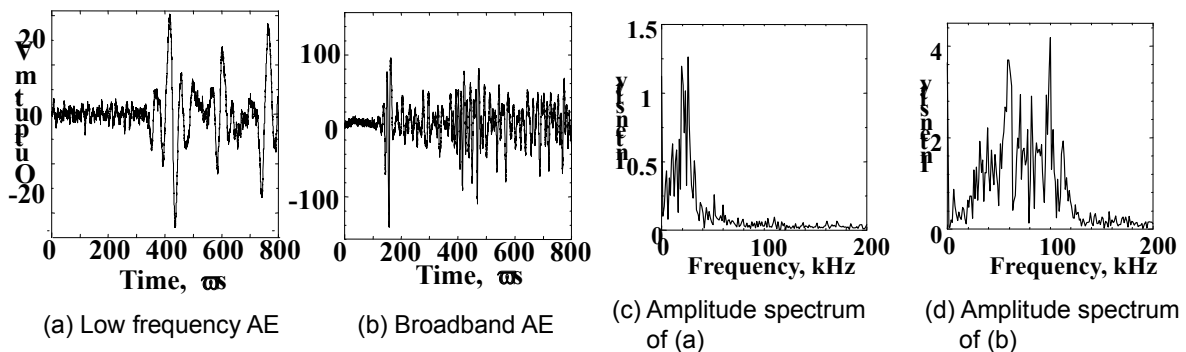


Fig. 5 Classified AE signals detected during the brazing process and their amplitude spectra

heating and cooling processes, these AEs could have been produced by the friction between the sample and the two steel plates acting as pressing components or by the friction between the bolts and the two steel plates. Because the brazing foil would not be melted in the initial stage of heating, no cracks could be generated. Moreover, in the sample with no brazing foil, only low-frequency AE was detected during the heating and cooling processes.

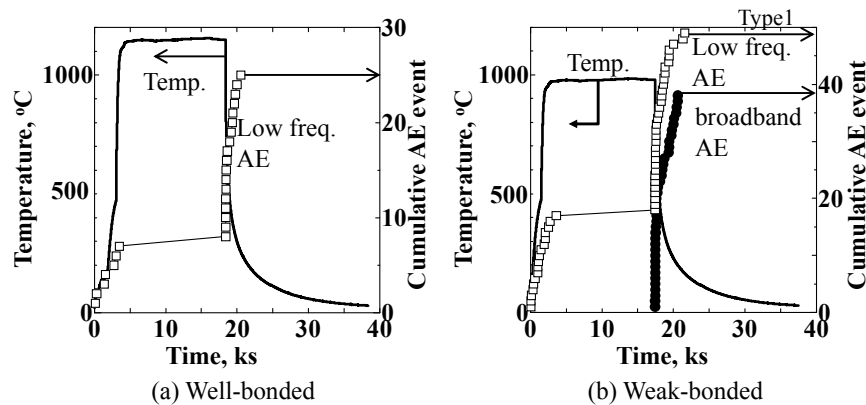


Fig. 6 Cumulative count of classified AE and temperature history

To verify our AE frequency classification, AE monitoring was performed while the sample was first heated to 950 °C, then cooled to 200 °C, and reheated to 1150 °C (which is proper brazing temperatures), and finally cooled to room temperature. Figure 7 shows typical AE waveforms during testing. In this test, the two types of AE signals were observed, which had similar frequency characteristics to the previous AEs, as shown in Fig. 5. Figure 8 shows the cumulative count of AE signals classified by frequency. Low-frequency AE signals corresponding to the friction in the sample setup were detected during each heating and cooling periods. Broadband AE signals were detected only during the cooling and heating periods that occurred after reaching 950 °C. This is because during these cooling and heating periods, voids at the interface could appear and the thermal stress acting at the interface (due to differences between the thermal expansion coefficient in the brazing layer and the carbon steel plate) could create microcracks either in the vicinity of the voids or along the interface.

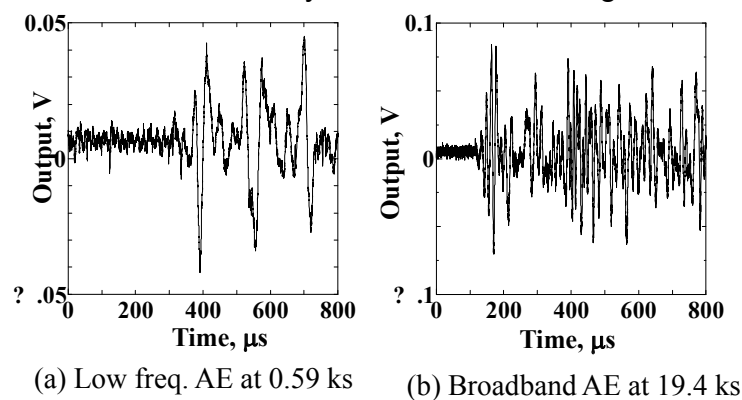


Fig. 7 Two types of AE signals during cyclic heating

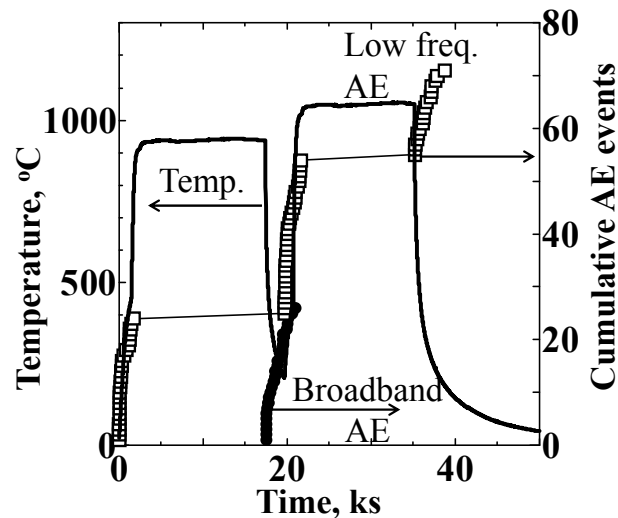


Fig. 8 Cumulative count of classified AE signals and temperature history for the sample under cyclic heating

4. Conclusions

Using a highly heat-resistant optical fiber (developed by plating an electroless Ni-P layer on a commercially available Cu-coated optical fiber), an optical AE monitoring system was developed. AE monitoring in a vacuum environment with temperatures of above 1000 °C was performed with the developed system to estimate brazing quality. The results of this study are as follows:

- 1) Many voids at the interface between the brazing layer and the AISI 304 plate that was used as an adherend were observed in the sample brazed at 950 °C. These voids could have caused a reduction of the elastic modulus and hardness in the brazing layer, as measured by the indentation test. Bonding quality for the sample brazed at 950 °C was low.
- 2) Two different types of AE signals were detected and can be classified according to their frequency characteristics during the heating and cooling periods of the brazing process. Broadband AE (with a frequency range of 20 to 120 kHz) was detected during the cooling period only for the sample brazed at 950 °C, which is below proper brazing temperatures. Low-frequency AE signals, with frequencies around 20 kHz, were observed during heating and cooling periods for the samples brazed at both 950 °C and 1150 °C.
- 3) The broadband frequency AE, which was detected during the cooling period for the sample brazed at 950 °C, could have been caused by microcracks between voids or along the interface of the brazed layer; these microcracks were generated by the

thermal stress during temperature changes. On the other hand, low- frequency AE could be caused by the friction in the sample and/or a sample holding device.

Using the heat-resistant optical fiber AE monitoring system developed in this study, in situ estimating the bonding conditions in brazing process in a vacuum environment with high temperatures is possible.

REFERENCES

- Choudhry, A and Tandon, N (2000), "Application of acoustic emission technique for the detection of defect in rolling element bearing", *Tribology international*, **33**(1), 39-45
- Hase, A, Wada, M., Koga, T. and Mishina, H (2014), "The relationship between acoustic emission signals and cutting phenomena in turning process", *Int. J. Adv. Manuf. Technol.*, **70**(5-8), 947-955
- Nama, H., Tabaru, T., Akiyama, M, Miyashi, N., Hayano, T., and Cho, H. (2007), "High-temperature acoustic emission sensing using aluminum nitride sensor", *J. Acoustic Emission*, **25**, 107-114
- Xu, J., Pickrell, G., Wang, X., Peng, W., Cooper, K. and Wang, A. (2005), "A novel temperature-insensitive optical fiber pressure sensor for harsh environment", *IEEE photonics technology letters*, **17**(4) 870-872
- Fomitchov, P.A., Kim, Y.K., Kromine, K.K., Krishnawamy, S. (2002), "Laser ultrasonic array system for real-time cure monitoring of polymer-matrix composite", *Jour. Composite materials*, **36**(15), 1889 - 1900]
- Hayano, T., Matsuo, T., Cho, H and Takemoto, M. (2007) "Heat resistant optical fiber system for monitoring AE in High temperature vacuum chamber", *Proc. The sixth international conference on acoustic emission*, 23-33
- Cho, H., Arai, R. and Takemoto, M. (2005), "Development of stabilized and high sensitive optical fiber acoustic emission sensor and its application", *J. Acoustic Emission*, **23**, 72-80
- Cho, H., Naruse T., Matsuo T. and Takemoto (2006), "Development of novel fiber AE sensor with multi-sensing function", *Key engineering materials*, **321-323**, 71-76